

However, a direct utilization of these methods for an on-line surveillance system is questionable because for unknown signals a high dynamic range of the registration equipment is necessary. The usefulness of electro-mechanical recording devices should not be overestimated as a component of an automatic surveillance system.

For the automatic analysis of weak boiling signals on a noisy background more sophisticated methods may be necessary to keep the numbers of spurious alarms in the allowable low range. Cross correlation technique (if more than one signal is available) or methods of pulse rate-assessment in the time domain may be helpful.

RESULTS OF INVESTIGATIONS WITHIN THE IWGFR BENCHMARK TEST ACOUSTIC BOILING NOISE DETECTION

H. MAUERSBERGER, K.-J. FRÖHLICH
Zentralinstitut für Kernforschung Rossendorf,
Akademie der Wissenschaften der DDR,
Rossendorf, German Democratic Republic

Abstract

The present paper deals with investigations of acoustic signals from a boiling experiment performed on the KNS I loop at KfK Karlsruhe. Signals have been analysed in frequency as well as in time domain. Signal characteristics successful used to detect the boiling process have been found in time domain. A proposal for in-service boiling monitoring by acoustic means is briefly described.

INTRODUCTION

One of the safety aspects of LMFBR's is the problem of local boiling in the reactor core. In order to prevent large-scale accident the failure should be detected in the earliest stage possible thus the probability of fault propagation is kept very low. Because of their potential for fast incipient failure detection acoustic methods became of growing interest (refs. 1, 2, 3). The analysis of acoustic data within the Benchmark on Sodium Boiling Noise Detection gives an opportunity to apply methods developed for water-to-sodium leak detection purposes to the aim of boiling detection.

The test signal has been measured during a boiling experiment performed on the KNS I loop at KfK Karlsruhe (ref. 4). With regard to the benchmark test the boiling signal has been heterodyned by the background signal measured with the same sensor in the same experiment. In order to get a various signal to noise ratio 12 files have been recorded. On each file the S/N ratio is decreased by about 2 dB. The duration time of each file is about 105 seconds. The onset of boiling in relation to the startup time of the file differs from file to file.

The aim of the benchmark test is to determine

- (i) the time of onset of boiling
- (ii) the time of increasing the boiling intensity
- (iii) the S/N discrimination achieved by participant's analysis technique.

SIGNAL ANALYSIS IN FREQUENCY DOMAIN

In order to get spectral characteristics of background and boiling noise, respectively, the power spectral densities (PSD) of the signals were calculated by means of an HP-Correlator with Spectrum Display (Fig. 1). Results of spectral analysis are given in Fig. 2. As a matter of fact, no specific boiling resonances could be found. The spectral characteristic of the acoustic signals obviously seems to be determined rather by properties of the sound-transmission enclosure and the measuring chain (i. e. geometry of the reactor and properties of waveguide with accelerometer, respectively) than by typical boiling phenomena. The absence of boiling-induced resonances can also be interpreted by a simple model of signal generation originally derived for signal evaluation in the case of sodium/water reactions in steam generators (ref. 5).

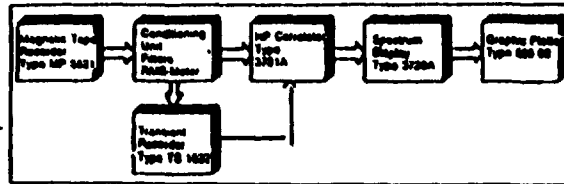


Fig. 1. Schematic diagram of spectrum analysing system

For more detailed information the spectra of single bursts have been compared with background noise (Fig. 3). There are again no boiling resonances but the difference in the PSD's magnitude of background and boiling noise becomes more evident. This fact has been used in deriving signal characteristics suitable for in-service boiling monitoring. Furthermore, signal analysis in the high frequency range has the advantage of suppressing unavoidable noise, e. g. from sodium flow and pumps.

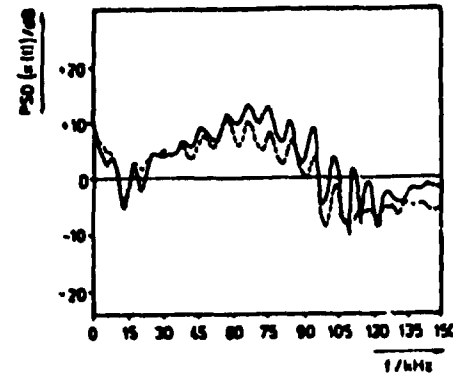


Fig. 2. PSD's of $x(t)$ of background (---) and boiling noise (—) using file 1 of test data

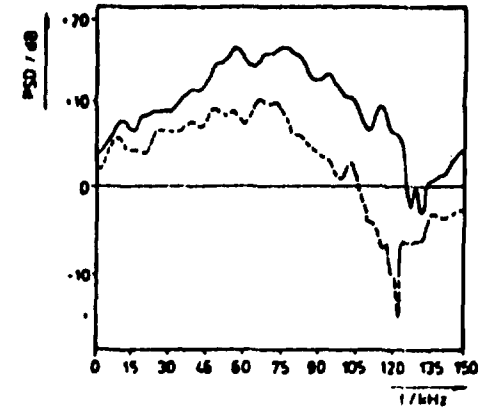


Fig. 3. Comparison of PSD's of a single burst (—) with the background (---)

SIGNAL ANALYSIS IN TIME DOMAIN

A typical boiling signal $x(t)$ and the corresponding elementary signal power $r(t)$, e. g. the r.m.s.-signal

$$r(t) = \sqrt{\frac{1}{T_r} \int_0^{t+T_r} x^2(t') dt'} \quad (1)$$

(T_r being the time constant of the r.m.s.-meter) are plotted simultaneously in Fig. 4. The background noise is superimposed by a random sequence of burst-like pulses. The difference in the signal properties of the "boiling" and "no boiling" state becomes more clear

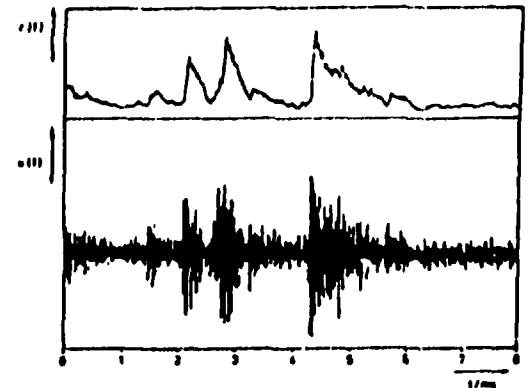


Fig. 4. Typical boiling-induced signals $x(t)$ and corresponding r.m.s.-signal $r(t)$

with the help of probability density functions (PDF) of the signal itself and the momentary signal power, respectively. With the onset of boiling the Kurtosis of the PDF of the acoustic signal $x(t)$ increases (Fig. 5). Comparing the "boiling" with the "no boiling" distribution this fact leads to a change of the skewness of the PDF of the momentary acoustic power $r(t)$. There is a considerable non-symmetry in the boiling distribution (Fig. 6). This is due to the occurrence of bursts in the boiling state. The same tendency (Fig. 7) can be observed even in the case of file 12 of the benchmark data (lowest boiling intensity) after 80 KHz high pass filtering.

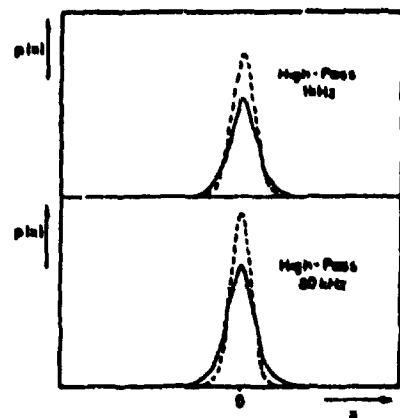


Fig. 5. PDF's of $x(t)$ of background (---) and boiling noise (—) filtered with 1 KHz and 80 KHz high pass, respectively (file 1 of test data)

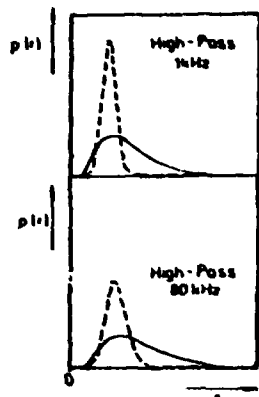


Fig. 6. PDF's of $r(t)$ in the case of file 1 ($x(t)$ filtered as given in Fig. 5)

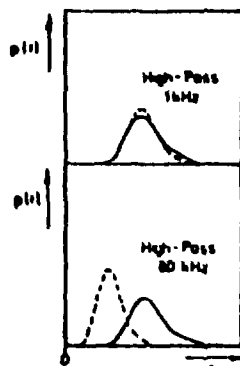


Fig. 7. PDF's of $r(t)$ using file 12

As derived in earlier reports (refs. 5, 6) analysis of r.m.s.-signals in time domain offers the possibility to distinguish background from "effect noise" in the presence of burst-like signals. Here, the time constant of the r.m.s.-meter has to be chosen in the same order of magnitude as the reverberation time of the sound-transmitting enclosure, because the trailing edge of the bursts is mainly governed by that characteristic. Otherwise, a deformation of the pulse shape and, consequently, detection errors can be expected. For the benchmark signals the reverberation time of about 100 μ s has been determined analysing the pulse shape.

In Fig. 8 several signal characteristics are plotted versus time using File 1 of the test data. It can be seen from the e-marked r.m.s.-signal that the onset of boiling gives rise to a certain increase in the signal level. On the other hand, the variance σ_r^2 of the r.m.s.-signal increases strongly due to the boiling-induced bursts. These effects

may also be caused by increasing the reactor power, changes of sodium flow, and changes in the signal gain, respectively. In order to avoid this disadvantage, a dimensionless measure of the signal roughness is introduced (b):

$$K = \frac{\sigma_r^2}{\bar{r}^2} \quad (2)$$

(\bar{r} being the mean value of the r.m.s.-signal).

Another signal characteristic successfully used is the pulse rate Z (c).

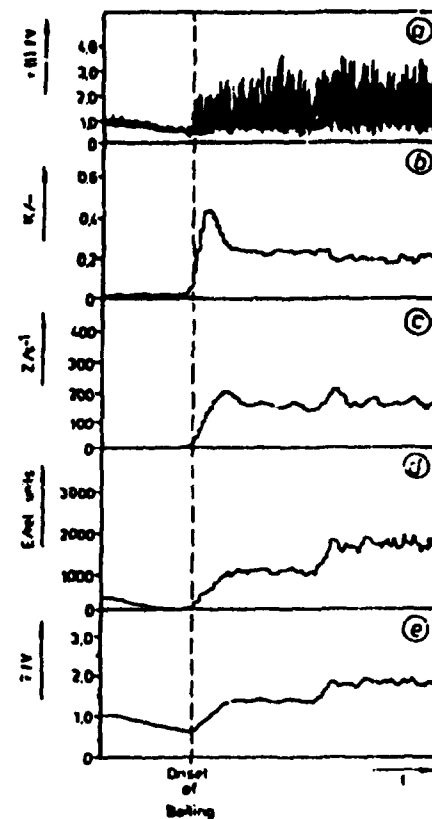


Fig. 8. Signal characteristics at onset of boiling

Z represents the number N of bursts during a measuring time T_M generated by discrimination of the r.m.s.-signal against a sliding threshold controlled by the r.m.s.-mean \bar{r} :

$$Z = \frac{N}{T_M} \quad (3)$$

A signal characteristic E (⊙) usual applied for detection of acoustic emission events (ref. 7) has been found suitable for boiling detection, too. This characteristic is a measure of burst energy Q_E during the measuring time

$$E = \frac{Q_E}{T_M} \quad (4)$$

In both Z- and E-measurements the choice of a proper threshold is an important task. According to results of PDF analysis (see Figs. 6 and 7, respectively) one has to evaluate in particular the tail area of the distribution. It has been shown (ref. 5) that it is possible to optimize this threshold getting in such a manner a more objective criterion for suitable values.

As in our evaluations of the benchmark data E-measurements are usually performed with the acoustic signal $x(t)$. In order to avoid misinterpretations one should apply this type of analysis to the r.m.s.-signal normalized by the mean value \bar{r} , too. An example using file 12 of the test data is given in Fig. 9. Because the physical interpretation is not yet clear this characteristic has not been included into the results so far. Finally it should be mentioned that in the case of a strong boiling state the mean value \bar{r} of the r.m.s.-signal can be used for detection purposes, too (see e-marked curve in Fig. 8) if one can ensure that the signal power increase is not caused by other effects.



Fig. 9. Measure of burst's energy derived from the r.m.s.-signal (t_{0B} and t_{1B} being the time of onset of boiling and of increasing the boiling intensity, respectively)

ANALYSIS OF BENCHMARK DATA

A scheme of the signal processing system is given in Fig. 10. The acoustic signals from the magnetic tape are filtered according to the results of PSD-analysis.

Further signal analysis has been performed in two different ways. On signal path I the filtered time signal $x(t)$ is preprocessed in the r.m.s.-meter the time constant of which is 100 μ s.

Further signal processing is performed by special units thus generating the signal characteristics K and Z. Flow sheets of the K- and Z-units are given in Fig. 11 and Fig. 12, respectively. The main elements of both units, such as integrator, squarer, divider, and counter are controlled by a microprocessor.

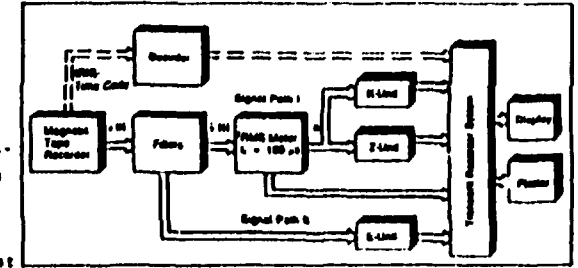


Fig. 10. Principle scheme of the signal analysing system

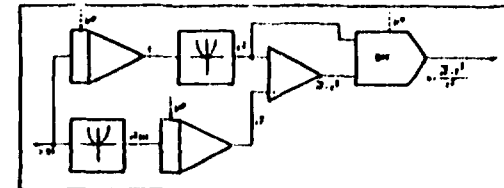


Fig. 11. Diagram of K-meter

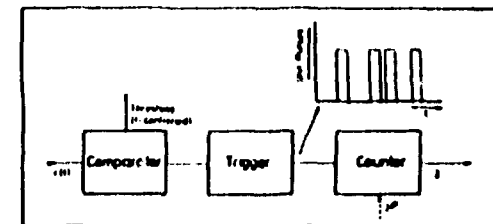


Fig. 12. Principle of the pulse rate meter

On signal path II the filtered signal is fed to the E-unit which was realized by a commercial available analyzer (ref. 8). The signal characteristics then are stored by means of a transient recorder (ref. 9) connected to which are a graphic plotter and a display. For plotting the signal characteristics versus real time either the IRIG Time Code or the 'Systron Donner' have been decoded and stored in the recorder, too.

The results of our analysis by the described processing system are given in Appendix A and B, respectively. For each data file the onset of boiling t_{OB} as well as the increasing boiling intensity t_{IBI} can be detected. Even in the case of file 12 there is a S/N discrimination of 9 ... 24 dB depending on the characteristic chosen.

As a rule, in both K- and Z-measurements the S/N discrimination decreases with decreasing S/N-ratio of the signals. Furthermore, detection of increasing boiling intensity is nearly impossible by K and Z, respectively. This seems to be caused by the increasing signal level in that state. Contrary to this, increasing of boiling intensity is clear detectable by E-measurement. Here, the S/N-discrimination increases slowly with decreasing S/N-ratio of the signals (files 1 ... 5) and remains then constant although the boiling intensity decreases (files 6 ... 12). This fact has not yet been understood and is still under investigation.

ACOUSTIC BOILING MONITORING SYSTEM

The given boiling detection conception might be realized by a microprocessor-based automatic boiling detection system. This system should consist of the following main parts:

- (i) Transducers mounted on waveguides, or sodium-immersible transducers
- (ii) Pre-amplifiers arranged near the reactor
- (iii) Signal processing unit in the control room of the plant.

The system should accomplish the following tasks:

- (i) Conversion of acoustic signals into electric ones
- (ii) Amplification and transmission of signals
- (iii) Signal filtering and preprocessing

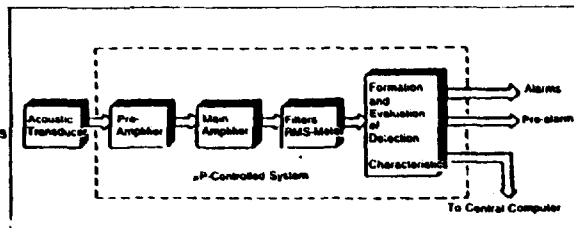


Fig. 13. Proposal for an acoustic boiling monitor

- (iv) Formation of detection characteristics K , Z , E , and \bar{F}
- (v) Generation of alarms
- (vi) Periodic self-checking
- (vii) Communication with a central computer.

A principle scheme of the system proposed is given in Fig. 13.

CONCLUSIONS

The results of analysing the Benchmark Test Data demonstrate that boiling detection by acoustic means is possible even in the case of very low boiling intensity. The proposed boiling monitor might be the first step in realizing a reliable boiling surveillance system.

As experienced from the BOR60 experiments a more effective boiling inspection can be carried out with simultaneous on-line monitoring both acoustic r.m.s.-signal and the neutron noise (ref. 10).

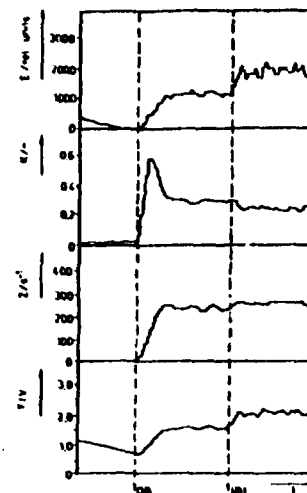
Furthermore, one has to state that results gained with artificial mixed data cannot be transferred simply to signals received from an original reactor in a nuclear power plant. Moreover, for a certain type of reactor it might be necessary to simulate boiling and to estimate the needed signal characteristics as a function of boiling intensity. With the knowledge of these characteristics optimum discrimination thresholds and other detection parameters (as alarm settings, measuring time interval, minimum detectable boiling intensity during a given detection time interval) can be determined.

REFERENCES

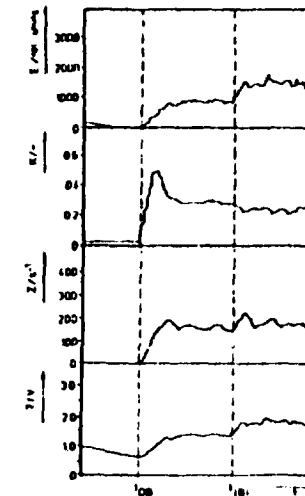
1. DAWSON, D. G., Acoustic detection of coolant boiling in the Dounreay fast reactor by transic time analysis during special fuel experiments, IAEA-IVGFR Specialist's Meeting on Boiling Noise Detection, Chester, England, June 9-11, 1981
2. ABERLE, J., et al., Potential and problems of acoustic boiling detection, 10th Meeting of the LMBWG, Karlsruhe, October 27-29, 1982
3. PRIDDHL, E., et al., Acoustic monitoring of LMFBR components, IAEA Seminar on Diagnosis of and Response to Abnormal Occurrences at NPP, Dresden, June 12-15, 1984

4. MUBER, F., et al., Temperature Distribution and Local Boiling behind a central Blockage in a Simulated FBR-subassembly. Int. Meet. on Fast Reactor and related Physics, Oct 1976, Chicago
5. PRIDDM, E., Akustische Detektion von Wasserlecks in natriumbeheizten Dampferzeugern unter Verwendung von Methoden der statistischen Entscheidungstheorie. Report ZfK-428 (1960)
6. MAJERSBERGER, H., Detektion zufälliger Impulsfolgen in Rauschsignalen zum Nachweis von Wasserlecks in natriumbeheizten Dampferzeugern. Report ZfK-529 (1984)
7. RAO, G. V., et al., Development of 'Acoustic Emission-Flaw Severity' relationships for the in-service monitoring of nuclear pressure vessels. Proc. of the 3rd Int. Conf. on Non-Destructive Evaluation in the Nuclear Industry, Salt Lake City, Utah, February 11-13, 1980
8. Product Data of Acoustic Emission Pulse Analyzer, Type 4429 (Brüel & Kjaer)
9. Beschreibung des Transientenspeichers TS 1622 (Labor für Elektrophysik, Dresden)
10. AFANASIEV, V. A., et al., The BOR60 sodium boiling experiment. Kernenergie 22 (1979)

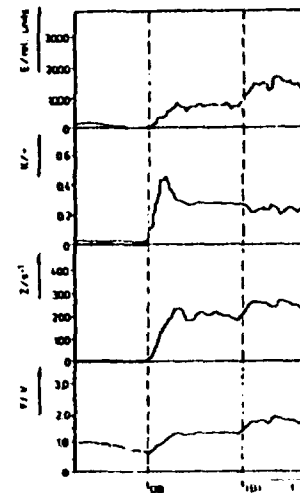
Appendix A



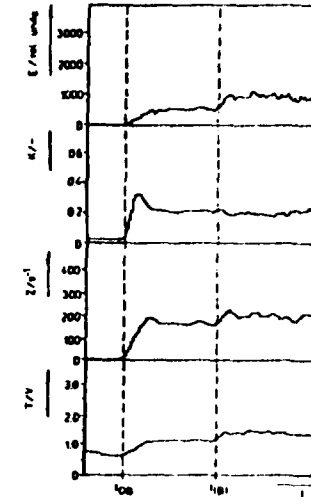
File 1



File 2

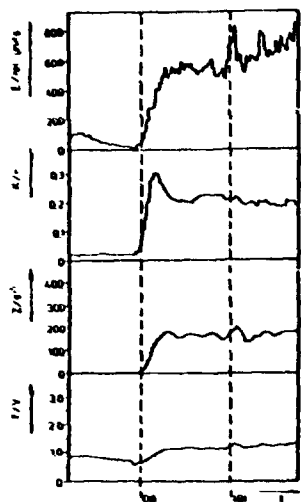


File 3

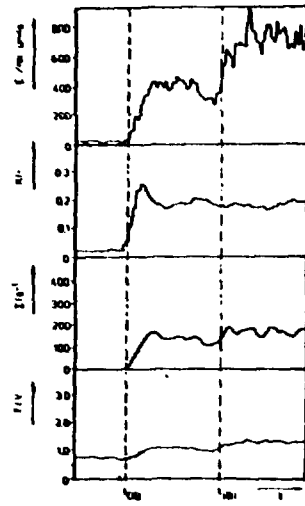


File 4

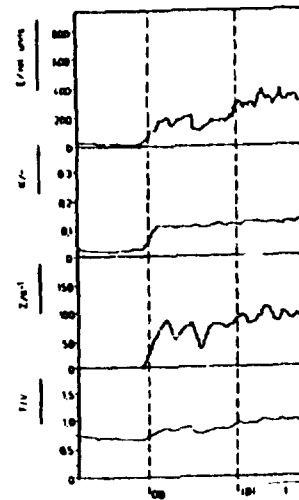
Fig. A1 - A4. Detection characteristics E, K, Z, and T/V plotted versus time



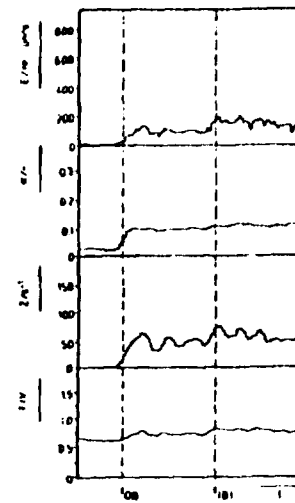
File 5



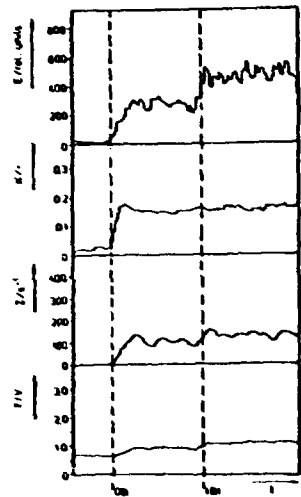
File 6



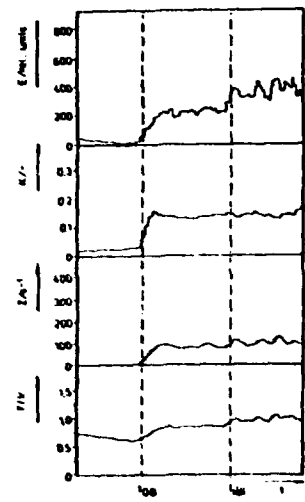
File 9



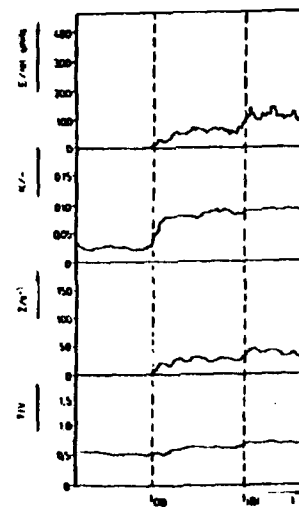
File 10



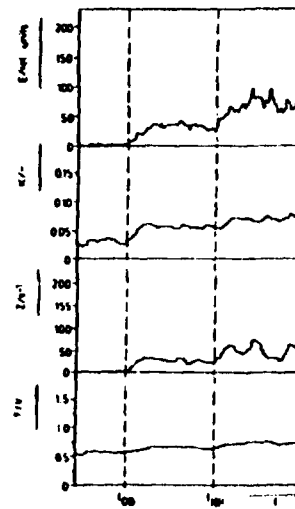
File 7



File 8



File 11



File 12

FIG. A5 - A8. Detection characteristics E, K, Z, and T plotted versus time

FIG. A9 - A12. Detection characteristics E, K, Z, and T plotted versus time

Appendix B

Table 3 Time of onset of boiling, of increasing boiling intensity, and the S/N-discrimination for each file

File	Time of Onset of Boiling	Time of Increasing the Boiling Intensity	S/N-Discrimination/dB		
			At Onset of Boiling		At Increasing Boiling Intensity
1	11 ^h 49' 47"	11 ^h 50' 27"	12	(E)	17
			30	(K)	24
			41	(Z)	43
2	12 ^h 05' 40"	12 ^h 06' 20"	11	(E)	18
			29	(K)	24
			38	(Z)	39
3	12 ^h 11' 44"	12 ^h 12' 24"	12	(E)	18
			28	(K)	24
			40	(Z)	42
4	12 ^h 25' 35"	12 ^h 26' 15"	13	(E)	19
			26	(K)	21
			39	(Z)	40
5	15 ^h 02' 38"	15 ^h 03' 18"	15	(E)	17
			24	(K)	20
			38	(Z)	39
6	15 ^h 15' 18"	15 ^h 15' 58"	23	(E)	27
			22	(K)	19
			38	(Z)	39
7	16 ^h 09' 24"	16 ^h 10' 04"	24	(E)	27
			19	(K)	19
			35	(Z)	36
8	16 ^h 16' 27"	16 ^h 17' 07"	22	(E)	25
			18	(K)	18
			34	(Z)	34
9	16 ^h 21' 39"	16 ^h 22' 19"	19	(E)	24
			16	(K)	16
			32	(Z)	33
10	16 ^h 32' 06"	16 ^h 32' 46"	20	(E)	25
			14	(K)	14
			30	(Z)	31
11	16 ^h 37' 46"	16 ^h 38' 26"	22	(E)	27
			12	(K)	13
			26	(Z)	28
12	16 ^h 48' 05"	16 ^h 48' 45"	20	(E)	24
			9	(K)	10
			22	(Z)	24

FIRST YEAR PROGRESS REPORT ON THE CO-ORDINATED RESEARCH PROGRAMME ON SIGNAL PROCESSING TECHNIQUES FOR SODIUM BOILING NOISE DETECTION

O.P. SINGH, R. PRABHAKAR, T.M. JOHN, R.K. VYJAYANTHI,
C.P. REDDY, M.V. PARIKH, S. PONPANDI
Indira Ghandi Centre for Atomic Research,
Kalpakkam, Tamil Nadu, India

Abstract

The present paper deals with investigations of acoustic signals from a boiling experiment performed on the MNS I loop at KFA Karlsruhe. Signals have been analysed in frequency as well as in time domain. Signal characteristics successfully used to detect the boiling process have been found in time domain.

1.0 INTRODUCTION

In Liquid Metal Fast Breeder Reactors (LMFBRs), detection of sodium boiling in its incipient stage itself is an important requirement from safety considerations. Sodium boiling in an LMFBR core can be broadly classified into integral and local boiling. The former may occur due to loss of flow or large blockages in subassemblies and can be detected by transducers/sensors available in the plant to monitor its steady state. Local boiling, which is more probable, arises as a result of small localised blockages within a subassembly due to build up of deposits in fuel channels over a period of time. This type of boiling remains undetected by sensors monitoring the plant steady state and special detection techniques are needed. During local boiling, acoustic noise is emitted due to generation, growth and collapse of sodium vapour bubbles and detection of local boiling